

# Nanodimensional Organostannoxane Molecular Assemblies

VADAPALLI CHANDRASEKHAR,\*

KANDASAMY GOPAL, AND

PAKKIRISAMY THILAGAR

Department of Chemistry, Indian Institute of Technology, Kanpur, Kanpur 208 016, India

Received December 21, 2006

## ABSTRACT

Organostannoxane cages, clusters, and coordination polymers containing  $[\text{Sn}_2(\mu\text{-O})]$ ,  $[\text{Sn}_2(\mu\text{-OH})]$ ,  $[\text{Sn}_2(\mu\text{-O})_2]$ ,  $[\text{Sn}_2(\mu\text{-OH})_2]$ , and  $[\text{Sn}_3(\mu_3\text{-O})(\mu\text{-OR})_3]$  building blocks have been assembled by the reactions of organotin precursors with phosphonic, phosphinic, carboxylic, or sulfonic acids. Various synthetic methodologies including Sn–C bond cleavage reactions and *solventless* procedures have been utilized to generate several nanodimensional organostannoxane assemblies. The synthesis, structure, and structural interrelationship of these diverse organostannoxane compounds are discussed. The synthetic knowledge gained to prepare specific organostannoxane structural forms in high yields has been utilized for the construction of dendrimer-like molecules. These contain a central stannoxane core and a functional periphery. The functional periphery can be readily modulated to assemble photoactive, electroactive, or multisite coordinating molecules. The synthesis, structure, and potential uses of these compounds are discussed.

## Introduction

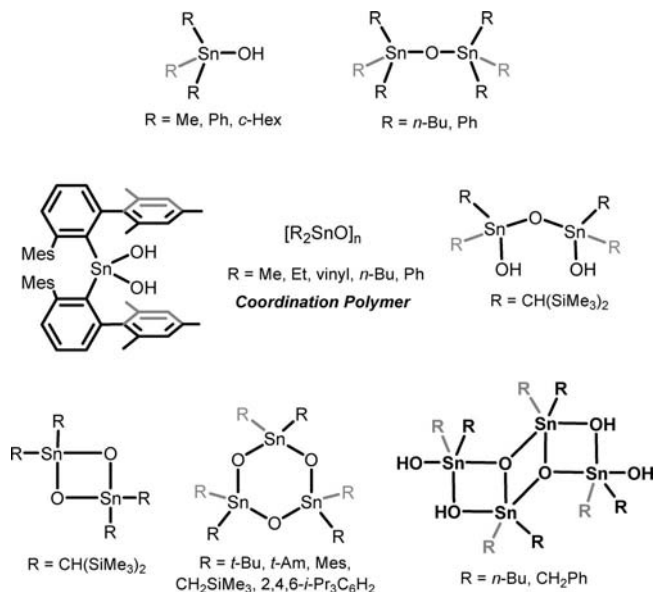
Organotin compounds are an important family of organometallic compounds and are receiving attention for several reasons. Many organotin compounds are used as reagents or catalysts in organic synthesis.<sup>1</sup> Stille reaction utilizes organotin compounds such as  $\text{R}_3\text{SnR}'$  (representative examples include  $n\text{-Bu}_3\text{SnPh}$ ,  $n\text{-Bu}_3\text{SnC}(\text{O})\text{CH}_2\text{CH}_3$ ,  $\text{Me}_3\text{SnPh}$ , and  $\text{PhSnCl}_3$ ) for the formation of new C–

Vadapalli Chandrasekhar was born in Calcutta (now Kolkata) in November 1958. He obtained his M.Sc. from Osmania University, India, in 1977 and his Ph.D. from the Indian Institute of Science, Bangalore, in 1982. After a postdoctoral stint at University of Massachusetts, Amherst, he worked at the Research Center of the Indian Petrochemicals Corporation Ltd. at Vadodara for a year. He then moved to Indian Institute of Technology, Kanpur, where he is currently the Lalit Kapoor Professor of Chemistry. He has won several awards such as the Shanti Swarup Bhatnagar Award (2003), Friedrich Wilhelm Bessel Research Award (2003), and Homi Bhabha Fellowship (1999–2000). He is a fellow of the Indian Academy of Science, Bangalore. His research interests are in the area of inorganic rings and polymers and main group organometallic chemistry.

Kandasamy Gopal was born in Salem, India, in 1978 and obtained his Masters degree at Pondicherry University, India, in 2001. He joined the research group of Prof. V. Chandrasekhar at the Indian Institute of Technology, Kanpur, in 2002, focusing on the study of structural diversity of organostannoxane compounds. His research interests include the synthesis of organostannoxane-based materials and their supramolecular assemblies.

Pakkirisamy Thilagar (born in 1976) grew up in Pondicherry, India. He completed his Masters in Chemical Sciences from Pondicherry University, India, in 2000. After working as a project assistant at the same university (2000–2002), he joined Indian Institute of Technology, Kanpur, where he is pursuing his Ph.D. under the supervision of Prof. V. Chandrasekhar. His research interests include inorganic rings and cages, nanoparticle self-assembly, and catalysis.

Chart 1. Triorganotin and Diorganotin Hydroxides and Related Condensed Products

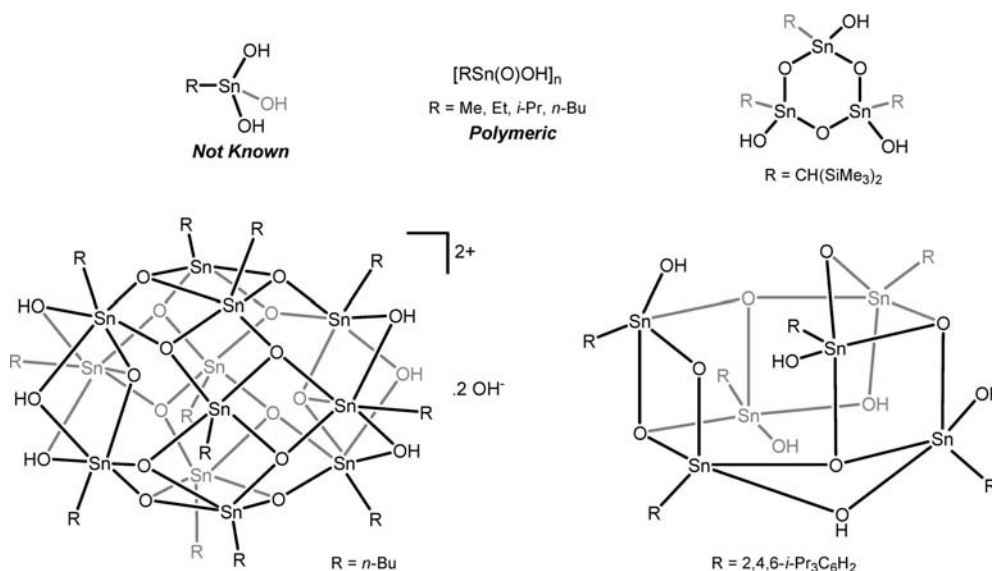


bonds and is a powerful tool in the synthetic repertoire of organic chemists.<sup>1</sup> Triorganotin radicals have been used widely in organic synthesis,<sup>1</sup> while diorganotin compounds have been used in esterification and transesterification reactions.<sup>2</sup> The use of diorganotin compounds in the stabilization of poly(vinyl chloride) is well-established.<sup>1</sup> In addition, many triorganotin compounds are used as fungicides and acaricides and in antifouling paints.<sup>1,3</sup> Some tri- and diorganotin compounds have been shown by *in vitro* studies to be active against a wide range of tumor lines.<sup>3</sup>

Among organotin compounds, organostannoxanes containing Sn–O units are a particularly interesting family.<sup>4</sup> Much of the interest in these compounds arises from the amazing structural diversity that they possess. The structural plasticity of organostannoxanes appears to be unique among the corresponding organometallic compounds of group 14 elements. Synthetic methodologies are now available that make it possible to design and assemble different types of organostannoxane cages and clusters.<sup>4</sup> This Account focuses, mainly, on our recent endeavors involving *large-sized nanodimensional* monoorganostannoxane compounds. For the sake of completeness, a few diorganotin compounds are also discussed. The synthetic strategies involved in the preparation of these organostannoxane assemblies, their structural features, and the structural interrelationship between different organostannoxane cages and clusters will be presented in this Account. Finally, we will also demonstrate how the knowledge of organostannoxane synthesis can be used in the construction of dendrimer-like molecules containing interesting peripheral groups that are photoactive or electroactive or multisite coordinating ligands.

\* To whom correspondence should be addressed. E-mail: vc@iitk.ac.in. Telephone: (+91) 512-259-7259. Fax: (+91) 512-259-0007/7436.

Chart 2. Monoorganotin Hydroxides and Related Condensed Products



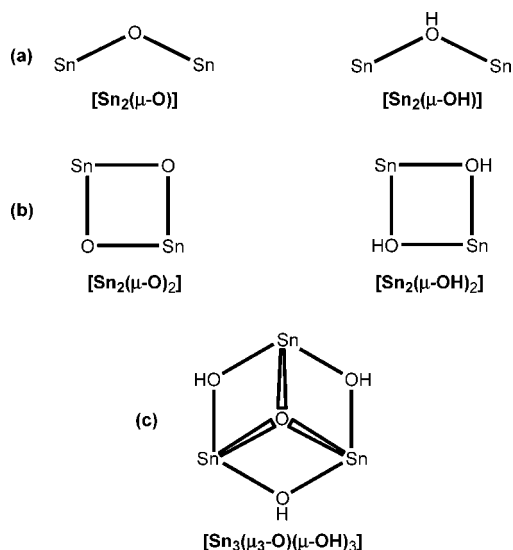
## Building Units of Organostannoxane Cages and Clusters

Although organostannoxane cages and clusters can be assembled by the use of a large variety of starting materials and by employing diverse routes including Sn–C bond cleavage reactions,<sup>5</sup> the most convenient synthetic precursors are organotin hydroxides and oxides (Charts 1 and 2). These can be elaborated into complex structural forms by reaction with an appropriate protic acid, such as  $\text{RCO}_2\text{H}$ ,  $\text{R}_2\text{P}(\text{O})\text{OH}$ ,  $(\text{RO})_2\text{P}(\text{O})\text{OH}$ ,  $\text{RP}(\text{O})(\text{OH})_2$ ,  $\text{RSeO}_2\text{H}$ , or  $\text{RSO}_3\text{H}$ .<sup>4</sup> In every case, the stannoxane cores of the resultant products are built by utilizing one or more of the three basic building blocks: (a)  $[\text{Sn}_2(\mu\text{-O})]$  and  $[\text{Sn}_2(\mu\text{-OH})]$ ; (b)  $[\text{Sn}_2(\mu\text{-O})_2]$  and  $[\text{Sn}_2(\mu\text{-OH})_2]$ ; (c)  $[\text{Sn}_3(\mu_3\text{-O})(\mu\text{-OH})_3]$  (Chart 3).

## Tetranuclear Cages (Containing $[\text{Sn}_2(\mu\text{-O})]$ ) and Coordination Polymers (Containing $[\text{Sn}_2(\mu\text{-OH})]$ Building Units)

We will begin this Account by considering the tetranuclear cages that contain the simplest of the building units, the  $[\text{Sn}\text{-O}\text{-Sn}]$  linkage. The first example of the tetranuclear cage,  $\{[(n\text{-BuSn})_2(\mu\text{-O})][\text{O}_2\text{P}(\text{OH})\text{-}t\text{-Bu}]_4\}_2$  ( $n\text{-Bu} = \text{-C}_4\text{H}_9$  ( $n$ -butyl);  $t\text{-Bu} = \text{-C}_4\text{H}_9$  ( $tert$ -butyl)) (**1**) was discovered by Holmes.<sup>6</sup> Our investigations on this reaction began with an examination of the reactions of  $[n\text{-BuSn}(\text{O})\text{OH}]_n$  and  $n\text{-BuSn}(\text{OH})_2\text{Cl}$  with  $t\text{-BuP}(\text{O})(\text{OH})_2$  and its silylated derivatives. All the reactions that we examined afforded exclusively the tetranuclear cage **1** (Scheme 1).<sup>7</sup> Such a remarkable preference for a single cluster type in varied reactions implies the rapid formation of a common intermediate. It was not possible for us to identify this species in these reactions. We turned our attention to obtaining analogous cages containing other substituents on tin. Benzyl- and allyltin compounds are known to undergo facile Sn–C bond cleavage reactions.<sup>5</sup> We have found that reactions of  $\text{Bn}_2\text{SnCl}_2$  or  $\text{Bn}_2\text{SnO}\cdot\text{H}_2\text{O}$  ( $\text{Bn} = \text{-CH}_2\text{C}_6\text{H}_5$  (benzyl)) with  $t\text{-BuP}(\text{O})(\text{OH})_2$  afford a mono-

Chart 3. Types of Stannoxane Building Blocks Found in Organostannoxane Compounds

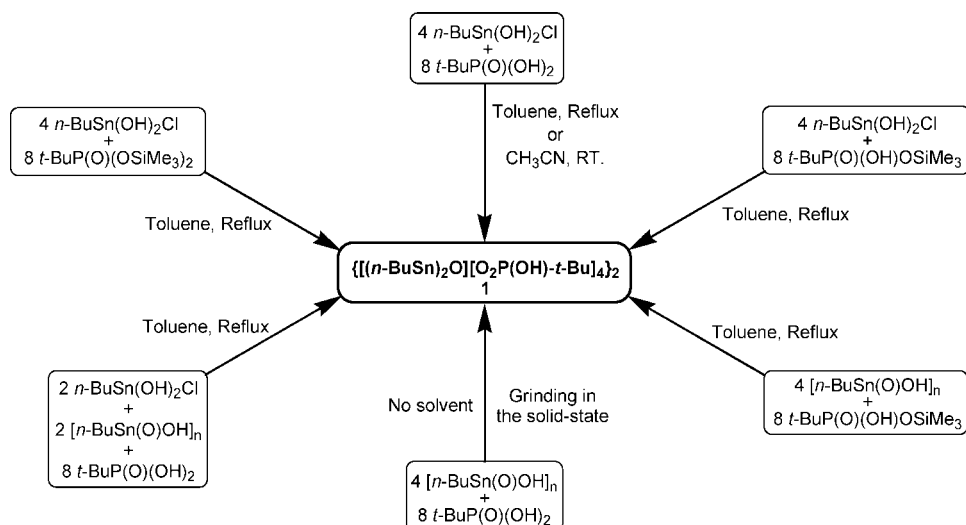


debenzylated product,  $\{[(\text{BnSn})_2(\mu\text{-O})][\text{O}_2\text{P}(\text{OH})\text{-}t\text{-Bu}]_4\}_2$  (**2**), which possesses an identical molecular structure to that of **1** (Scheme 2).<sup>8</sup> Use of  $\text{Bn}_3\text{SnCl}$  also affords **2** in a reaction that involves double debenzylation.

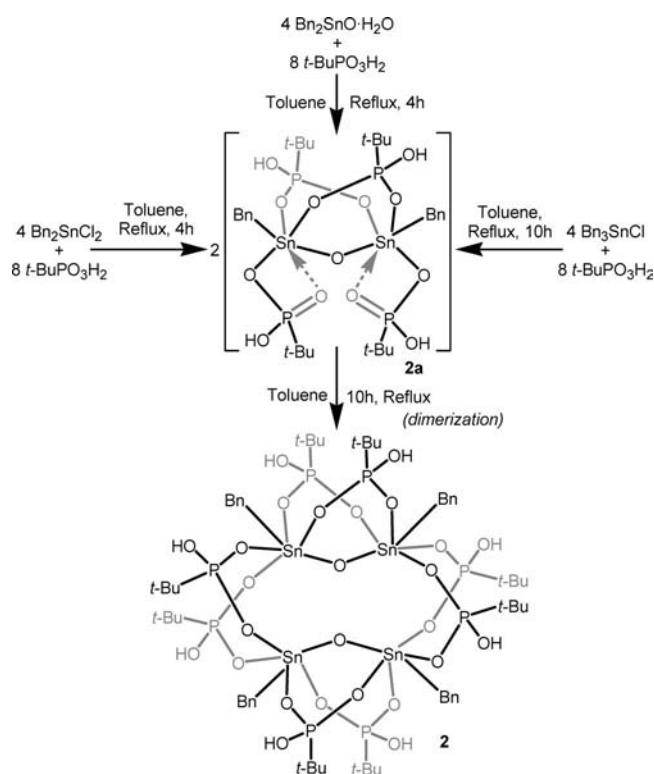
The  $^{119}\text{Sn}$  NMR of **2** shows a triplet of triplets with a chemical shift of  $-661.6$  ppm.<sup>8</sup> The analogous resonance for **1** occurs at  $-630.4$  ppm.<sup>6</sup> The formation of **2** can be monitored by NMR. Thus, the  $^{31}\text{P}$  NMR spectrum of the reaction mixture shows the initial formation of a half-cage intermediate, **2a**, with signals at 33.7 and 31.8 ppm, which eventually dimerizes to form the full-cage **2** over a period of time (Scheme 2).<sup>8</sup> The rapid formation of an analogous half-cage intermediate is responsible for the exclusive formation of **1** in various reaction conditions described above.

The molecular structure of **2** is made up of two  $[\text{Sn}\text{-O}\text{-Sn}]$  units (Figure 1). In each  $[\text{Sn}\text{-O}\text{-Sn}]$  unit, the two tin atoms ( $\text{Sn1}$  and  $\text{Sn2}$ ) are bridged by an oxygen atom ( $\text{O1}$ ) and by two bidentate  $[t\text{-BuP}(\text{OH})\text{O}_2]^-$  ligands

## Scheme 1. Ligand-Driven Assembly of the Tetranuclear Cage 1



## Scheme 2



(P1 and P2). This generates an open-book-shaped bicyclic ring, which is made up of two six-membered rings [Sn1–O1–Sn2–O12–P1–O11] and [Sn1–O1–Sn2–O21–P2–O22] with a dihedral angle of 68.51(2)°. The Sn–O bond distance within the [Sn–O–Sn] unit (Sn1–O1 and Sn2–O1) is 2.117(3) Å, while the Sn1–O1–Sn2 angle is 135.17(2)°. Two such [Sn–O–Sn] units are further bridged on either end by means of two pairs of bidentate [*t*-BuP(OH)<sub>2</sub>]<sup>−</sup> ligands (P3, P4, P3\*, P4\*) (Figure 1).

Debenzylation reactions need not be the only reaction course of benzytin compounds. Recently we have found that the reaction of Bn<sub>2</sub>SnCl<sub>2</sub> with pyrazole-3,5-dicarboxylic acid (L<sup>1</sup>H<sub>3</sub>) affords a two-dimensional coordination polymer {[ (Bn<sub>2</sub>Sn)<sub>3</sub>(μ-OH)(L<sup>1</sup>)<sub>2</sub>]<sub>2</sub>[Bn<sub>2</sub>SnCl]<sub>2</sub>]<sub>n</sub> (3) (Scheme

3).<sup>9</sup> The latter contains hexatin macrocycles interlinked to each other by Bn<sub>2</sub>SnCl groups (Figure 2a). It can be noted that all the Sn–Bn bonds in compound 3 remain intact. Each macrocycle repeating unit of 3 contains two tri-tin subunits where two tin atoms are held together by a μ-OH group. The macrocycle repeating unit of 3 is approximately rectangular in shape, and its dimensions are nanometric (Figure 2b). Hydrolysis of 3 in presence of pyridine affords a one-dimensional polymeric tape {[ (Bn<sub>2</sub>Sn)<sub>3</sub>(μ-OH)(L<sup>1</sup>)<sub>2</sub>(Py)<sub>2</sub>]<sub>2</sub>[ (Bn<sub>2</sub>Sn)<sub>2</sub>(μ<sub>3</sub>-O)(μ-OH)<sub>2</sub>]<sub>n</sub> (4) (Scheme 3). The robust nanodimensional macrocyclic repeat unit of 3 is retained in 4, while the bridging Bn<sub>2</sub>SnCl units have been transformed into the tetranuclear ladder, [(Bn<sub>2</sub>Sn)<sub>2</sub>(μ<sub>3</sub>-O)(μ-OH)<sub>2</sub>] units (Figure 2c).

In addition to the two- and one-dimensional coordination polymers discussed above, we have also been able to obtain a phosphinate-supported one-dimensional coordination polymer that contains a [Sn–OH–Sn] unit. Thus, the reaction of [*n*-Bu<sub>2</sub>SnO]<sub>n</sub> with 1,1,2,3,3-pentamethyltrimethylenephosphinic acid, *cyc*-P(O)(OH), affords {[ (n-Bu<sub>2</sub>Sn)<sub>2</sub>(μ-OH)(*cyc*-PO<sub>2</sub>)<sub>3</sub>]<sub>n</sub> (5) (Scheme 4).<sup>10</sup> Compound 5 is a coordination polymer that contains alternate eight- and six-membered rings where every tin atom is at the junction of a spirocyclic ring system.

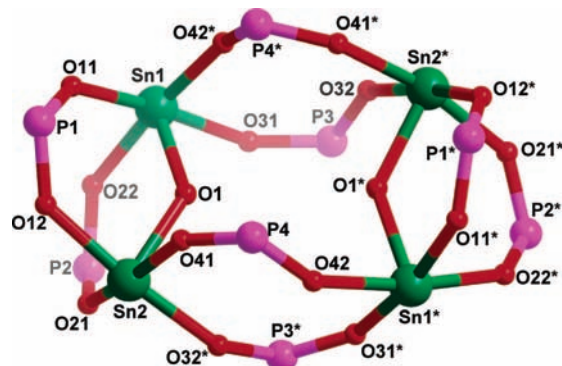
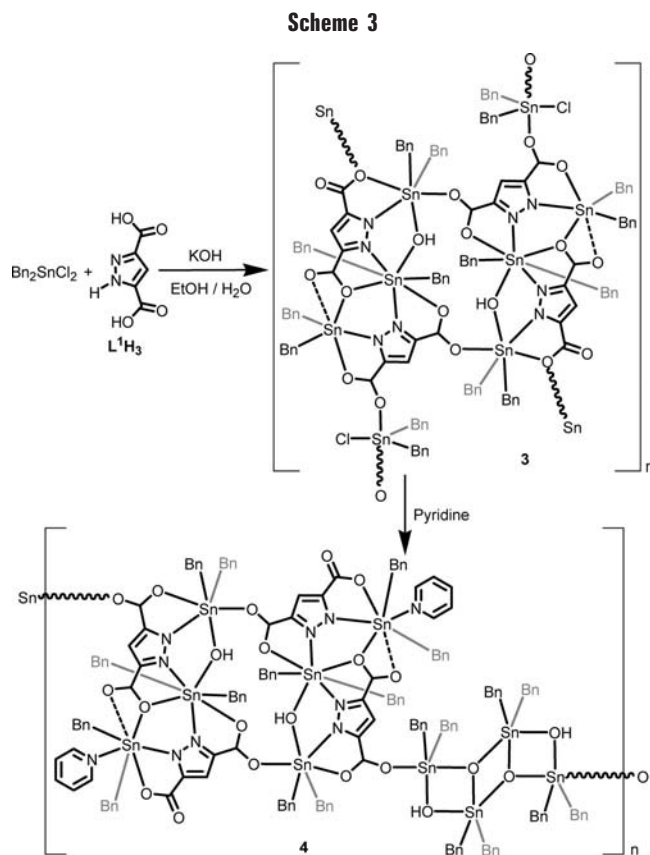
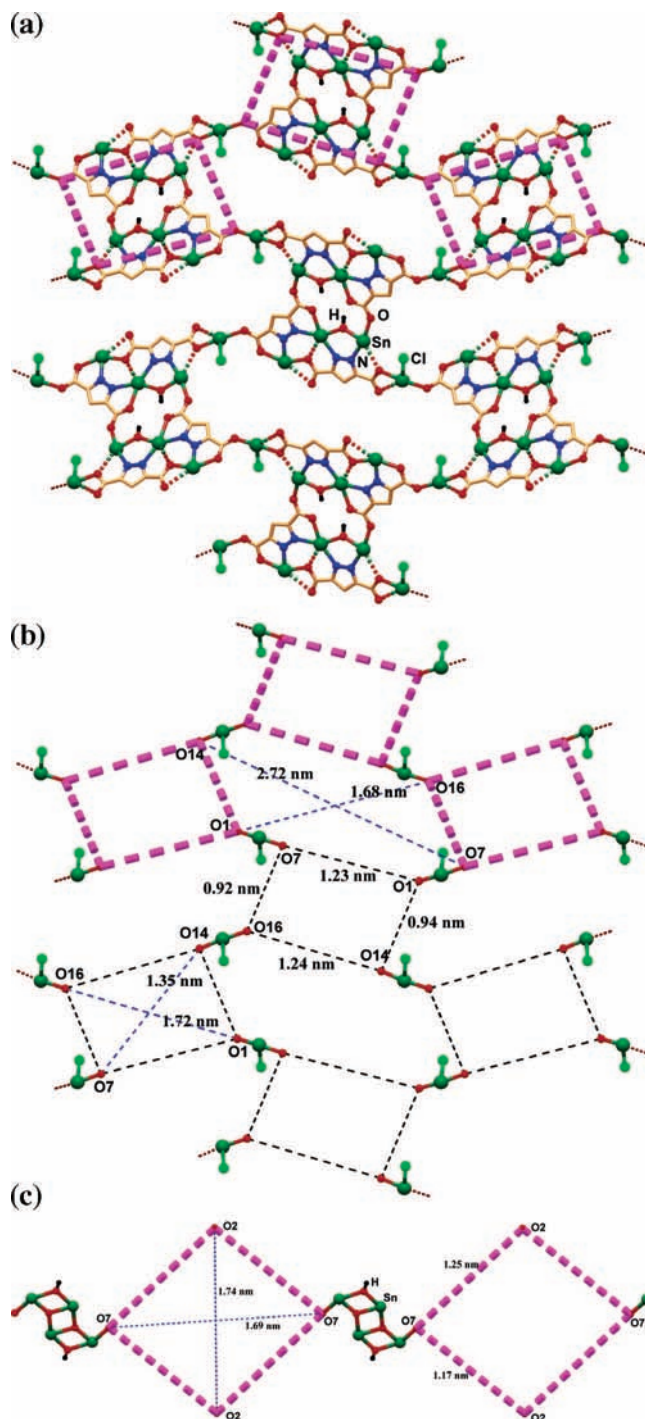


FIGURE 1. Organooxotin core of tetranuclear cage 2 shown along with the PO<sub>2</sub> part of the *t*-BuP(O)(OH)<sub>2</sub> ligand.



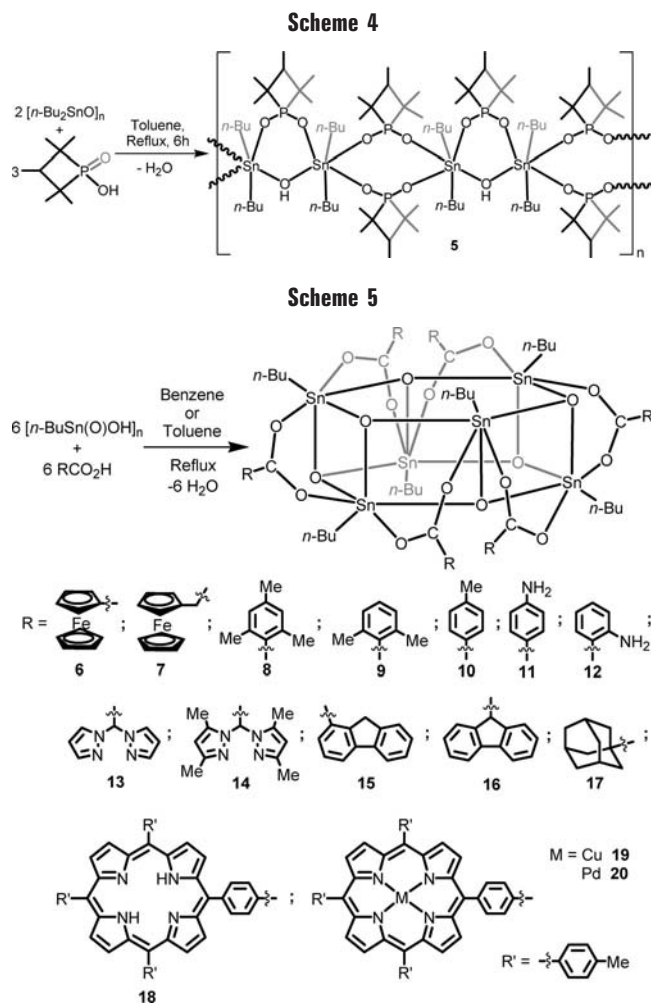
As mentioned above, the four-membered  $[\text{Sn}_2(\mu\text{-O})_2]$  rings constitute important building blocks for the construction of organostannoxane cages.<sup>4</sup> The most ubiquitous of such cages are the hexanuclear compounds,  $[\textit{n}\text{-BuSn}(\text{O})\text{O}_2\text{CR}]_6$ , also known as *drums*. Although, several synthetic routes are available for the preparation of these cages, the most convenient synthesis of this class of compounds is from a direct 6:6 reaction of the monoorganotin(IV)-hydroxide,  $[\textit{n}\text{-BuSn}(\text{O})\text{OH}]_n$ , with protic acids such as carboxylic acids.<sup>4</sup> This reaction is quite general as indicated by the synthesis of compounds **6–20** (Scheme 5).<sup>11</sup> The hexanuclear drums are also formed in reactions of  $[\textit{n}\text{-BuSn}(\text{O})\text{OH}]_n$  with phosphates of the type  $(\text{RO})_2\text{P}(\text{O})(\text{OH})$ .<sup>12</sup> Reactions of  $[\textit{n}\text{-BuSn}(\text{O})\text{OH}]_n$  with phosphinic acids,  $\text{R}_2\text{P}(\text{O})\text{OH}$ , are more complex and various products such as cubes, butterfly clusters, crowns, extended clusters and O-capped clusters are formed. These will not be dealt in this Account as this subject has been adequately covered elsewhere.<sup>4</sup>

Molecular structures of several organostannoxane drums reveal the following common features. All of them contain a central  $\text{Sn}_6\text{O}_6$  stannoxane core, which contains two puckered six-membered  $[\text{Sn}_3(\mu_3\text{-O})_3]$  rings as its top and bottom faces (Figure 3).<sup>11a</sup> On the other hand, the side of the drum contains six puckered four-membered  $[\text{Sn}_2(\mu_3\text{-O})_2]$  rings. Alternate tin atoms are held together by the coordination action of bidentate carboxylate groups. All



**FIGURE 2.** (a) Two-dimensional polymeric structure of **3**, (b) cartoon representation of the two-dimensional network of **3**, and (c) cartoon representation of the ladder bridged one-dimensional polymer **4**. In all cases, the rectangular boxes drawn in pink color represent the hexanuclear macrocyclic units.

the tin atoms of the drum compounds are chemically equivalent and a single chemical shift is seen in their  $^{119}\text{Sn}$  NMR at about  $-480.0$  ppm.<sup>11</sup> The structural features of various drum compounds are similar. In general, the Sn–O bond distances involving the  $\text{Sn}_6\text{O}_6$  core are shorter (average value for **6**,  $2.060(4)$  Å) in comparison to those found exo to the cage (average value for **6**,  $2.141(4)$  Å).<sup>11a</sup> The Sn–O–Sn bond angles in the six-membered rings are



wider (average value for **6**, 132.10(2)°) than those found in the four-membered rings (average value for **6**, 100.37(2)°).

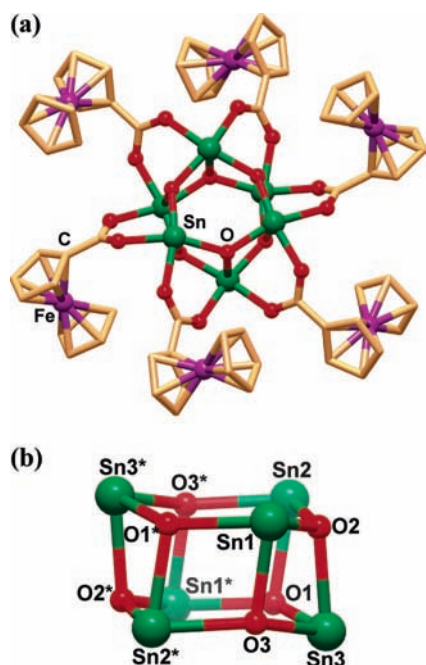


**FIGURE 3.** (a) Molecular structure of the hexaferrocenyl assembly **6** and (b) side view of the hexameric stannoxane core in **6** (all the  $\text{Sn}_2\text{O}_2$  and  $\text{Sn}_3\text{O}_3$  rings are puckered).

Many of the drum compounds exhibit rich supramolecular architectures in their crystal structures. Various noncovalent interactions including  $\text{O-H}\cdots\text{O}$ ,  $\text{C-H}\cdots\text{O}$ ,  $\text{C-H}\cdots\text{F}$ ,  $\text{C-F}\cdots\pi$ ,  $\text{C-H}\cdots\pi$ , and  $\pi$ -stacking interactions have been documented. The cumulative effect of such interactions is manifested in the form of one-, two- and three-dimensional supramolecular structures.<sup>11</sup> A representative example of such a supramolecular structure is shown in Figure 4.

In attempting to extend the range of organostannoxane cluster types, we investigated the reaction of  $[\text{n-BuSn}(\text{O})\text{OH}]_n$  with  $(\text{PhO})_2\text{P}(\text{O})\text{H}$ . The only product that we were able to isolate was a hexanuclear cage,  $\{[\text{n-BuSn}]_3(\mu_3\text{-O})(\mu\text{-OPh})_3(\text{HPO}_3)_2\}_2$  (**21**) (Scheme 6).<sup>13</sup> An in situ hydrolysis of  $(\text{PhO})_2\text{P}(\text{O})\text{H}$  affords phenol and the phosphonate ligand ( $\text{HPO}_3^{2-}$ ), which assist the formation of the cage **21**, also known as *double O-capped cluster*. A series of such hexanuclear cages (**22–24**) were synthesized in a direct reaction involving  $[\text{n-BuSn}(\text{O})\text{OH}]_n$  and  $\text{H}_3\text{PO}_3$  and various phenols (Scheme 6).<sup>14</sup>

The molecular structure of these cages is very similar and consists of two  $[\text{n-BuSn}]_3(\mu_3\text{-O})(\mu\text{-OR})_3$  subunits (Figure 5). A  $\mu_3\text{-O}$  (O1) is involved in bridging three tin atoms (Sn1, Sn2, and Sn3) in a capping coordination mode. Three phenoxide oxygen atoms (O8, O9, and O10) are involved in binding two adjacent tin centers. This concerted coordination action of the oxide and the phenoxide ligands results in the formation of three contiguous  $[\text{Sn}_2(\mu\text{-OPh})_2]$  four-membered rings to afford a  $\text{Sn}_3\text{O}_4$  building block (*O-capped tri-tin*, Chart 3). The average  $\text{Sn}-(\mu_3\text{-O})$  distance for **21** is 2.065(4) Å, while the average  $\text{Sn}-(\mu\text{-OPh})$  distance for **21** is 2.172(4) Å.<sup>13</sup> The solid-state structures of the double O-capped clusters **22–24** show interesting supramolecular architectures as a result of halogen bonding (Figure 6).<sup>14,15</sup>

### Hexanuclear Prismane Cage (Containing $[\text{Sn}_2(\mu\text{-OH})_2]$ Building Units)

$[\text{Sn}_2(\mu\text{-OH})_2]$  building units are also important in forming organostannoxanes.<sup>1,4,5</sup> For example, the reaction of  $(\text{Ph}_3\text{Sn})_2\text{O}$  with  $\text{R}_f\text{CO}_2\text{H}$  affords  $\{[\text{Ph}_2\text{Sn}(\mu\text{-OH})(\text{O}_2\text{CR}_f)]_2\}$  ( $\text{R}_f = 2,4,6\text{-}(\text{CF}_3)_3\text{C}_6\text{H}_2$ ) (**25**) (Scheme 7).<sup>16</sup> Compounds with analogous  $[\text{Sn}_2(\mu\text{-OH})_2]$  cores are obtained in the reaction of  $[\text{t-Bu}_2\text{SnO}]_3$  with carboxylic acids<sup>11f,11g,17</sup> (Scheme 7), as well as in the reactions of  $[\text{R}_2\text{SnO}]_n$  with  $\text{CF}_3\text{SO}_3\text{H}$ .<sup>18</sup>

In view of the limited structural types formed in the reaction between  $[\text{n-BuSn}(\text{O})\text{OH}]_n$  and carboxylic acids,<sup>4</sup> we probed the reaction of 9-hydroxy-9-fluorene-carboxylic acid ( $\text{L}^2\text{H}_2$ ). We anticipated that the presence of the geminal hydroxyl group in  $\text{L}^2\text{H}_2$ ,  $[\text{C}(\text{OH})\text{CO}_2\text{H}]$ , would provide an additional binding site that would lead to new product types. This was realized in the isolation of  $\{[\text{n-BuSn}(\mu\text{-OH})(\text{L}^2)]_6\cdot 3\text{H}_2\text{O}\cdot 2\text{CHCl}_3\}$  (**29**) (Scheme 8).<sup>19</sup> On the other hand, the reaction of  $[\text{n-BuSn}(\text{O})\text{OH}]_n$  with  $\text{L}^2\text{H}_2$  and 4-iodophenol affords  $\{[\text{n-BuSn}(\mu\text{-OH})(\text{L}^2)]_6\cdot 6\text{ROH}\cdot 6\text{H}_2\text{O}\cdot \text{CHCl}_3\}$  ( $\text{ROH} = 4\text{-iodophenol}$ ) (**30**) (Scheme 9). The molecular structures of **29** and **30** are very similar and

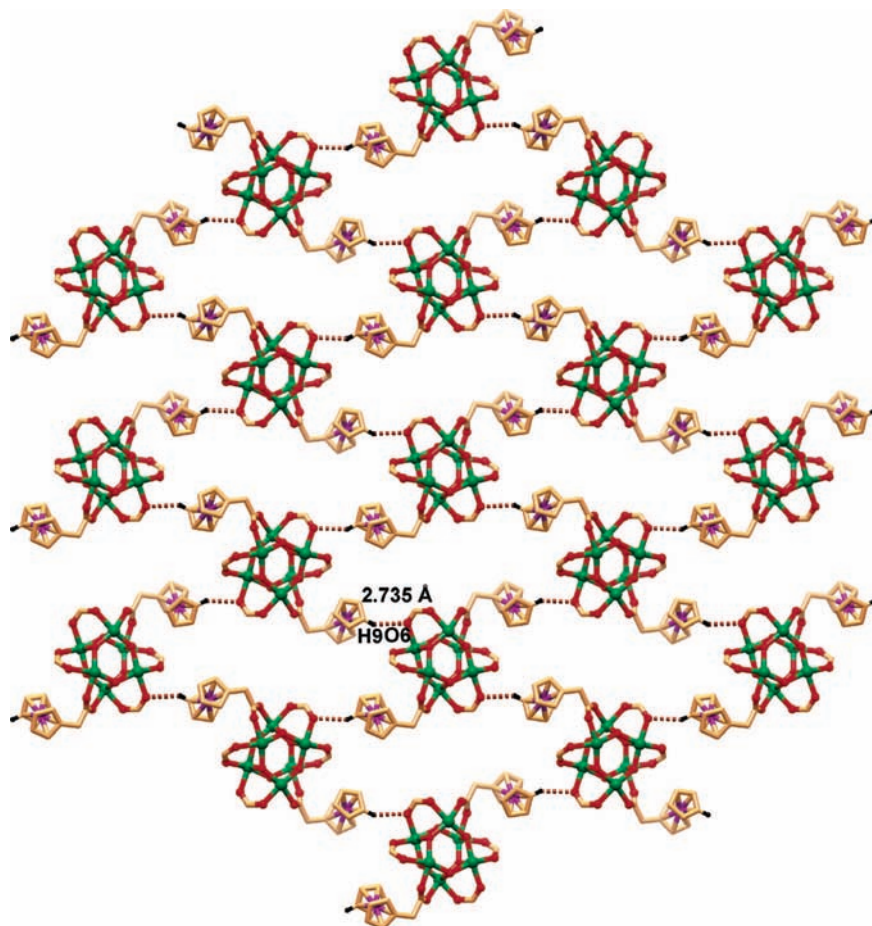
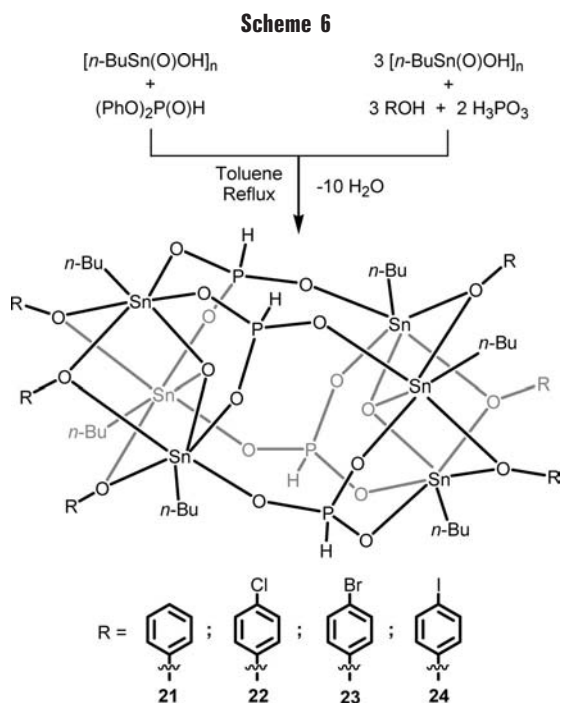


**FIGURE 4.** C–H···O hydrogen bonding mediated supramolecular assembly in the crystal structure of **7**. Reproduced with permission from ref 11b. Copyright 2002 American Chemical Society.



contain two centrosymmetrically related tri-tin subunits, which are held together by three  $[\text{Sn}_2(\mu\text{-OH})_2]$  units (Figure 7). Each of the three tin atoms of a subunit occupies the vertices of an equilateral triangle. Two such

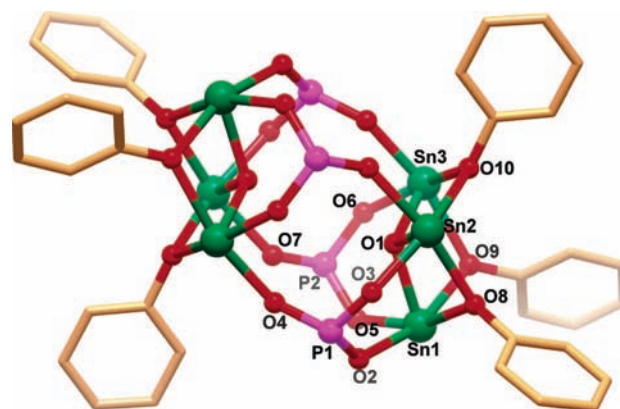


**FIGURE 5.** Molecular structure of the hexanuclear double O-capped cluster **21** (unlabeled atoms are symmetry-related to the labeled atoms).

equilateral triangles are joined to each other by six  $\mu\text{-OH}$  groups to afford the regular trigonal prism cage structures of **29** and **30**. The role of the ligands ( $L^2$ ) in holding the six tin atoms is very crucial. The carboxylate part of the ligand is involved in bridging two adjacent tin atoms, while the hydroxide part is bonded to one tin. The various Sn–O distances involved in the cage are very similar (Sn–OH 2.153(2), Sn–O 2.017(3), Sn–O 2.174(2) Å).

The crystal structure of **30** reveals the presence of a three-dimensional columnar supramolecular structure containing

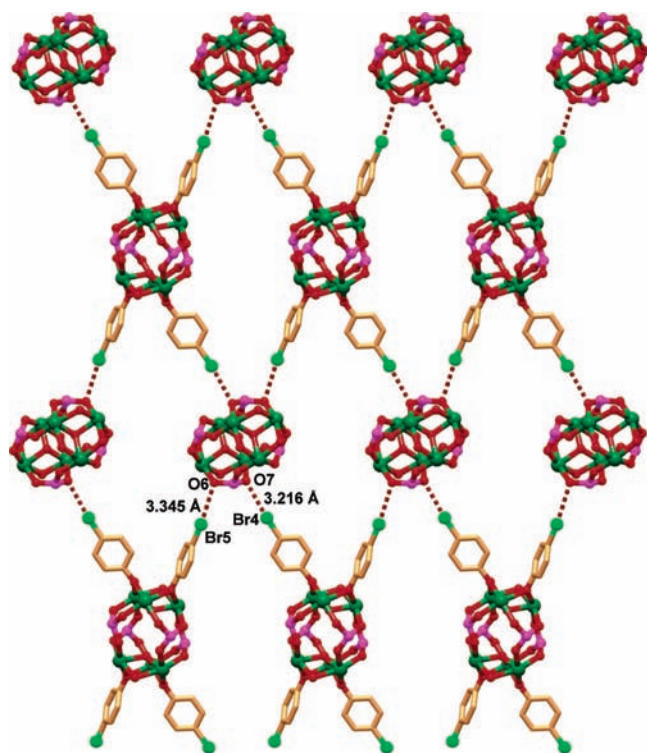


**FIGURE 6.** P–O···Br halogen bonding mediated two-dimensional supramolecular assembly in the crystal structure of **23** (alternate rows of bromine-donor and bromine-acceptor clusters). Reproduced with permission from ref 14. Copyright 2005 American Chemical Society.

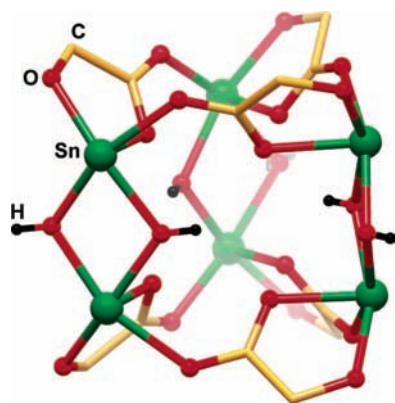
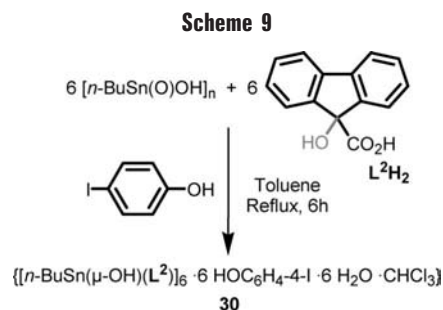
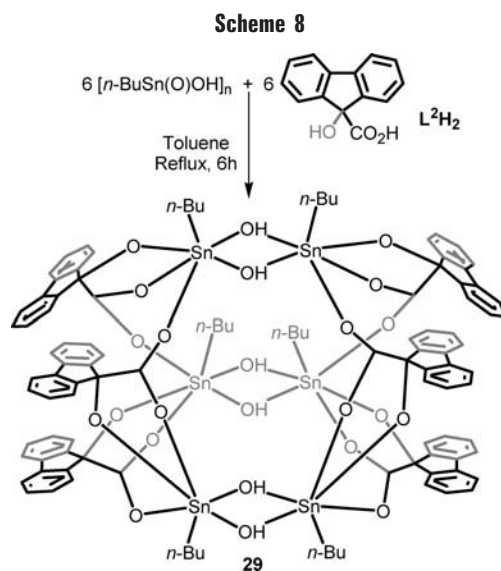
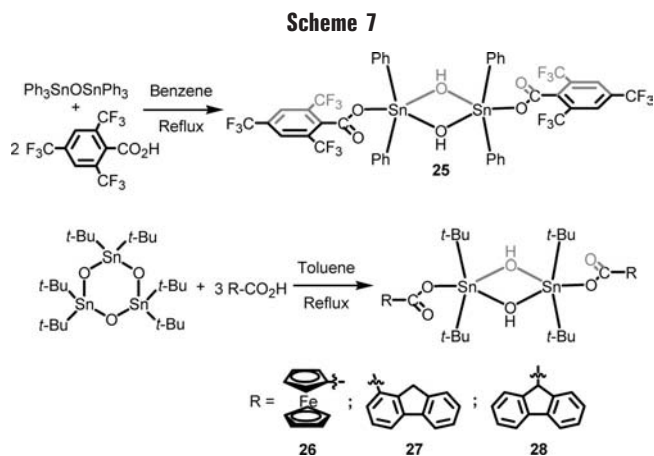


**FIGURE 7.** The core structure of the prismane cage **29**.

$C_3$  symmetric voids.<sup>19</sup> The diameter of these columns is about 10 Å. The interior lining of the column contains hydrophilic Sn–OH units and carboxylate oxygen atoms and hydrophobic *n*-butyl units. Because of the alternation of hydrophobic and hydrophilic regions, a discrimination of the guest molecules is achieved based on site-selective entrapment. Thus, chloroform molecules preferentially occupy the hydrophobic pockets, while phenol molecules bind to the hydrophilic region (Figure 8).

### Dodecanuclear Football Cage (Containing $[\text{Sn}_2(\mu\text{-O})_2]$ and $[\text{Sn}_3(\mu_3\text{-O})(\mu\text{-OH})_3]$ Building Units)

One of the condensation products of a putative  $\text{R}\text{Sn}(\text{OH})_3$  is the dodecanuclear football cage,  $\{[(n\text{-BuSn})_{12}(\mu_3\text{-O})_{14}(\mu\text{-OH})_6]^{2+} \cdot 2\text{OH}^-\}$ .



$\text{OH})_6]^{2+} \cdot 2\text{OH}^-$ .<sup>20</sup> The simplest synthesis of such cages involves the reaction of  $[(n\text{-BuSn}(\text{O})\text{OH})_n]$  with an arylsulfonic acids (Scheme 10).<sup>21</sup> The football structure of the macrocations in **32** consists of 12 tin atoms, which are linked by  $\mu_3\text{-O}$  and  $\mu\text{-OH}$  bridges.<sup>21</sup> All the *n*-butyl substituents attached to the tin atoms point away from the stannoxane core. Among the 12 tin atoms present in the molecule, three each are situated at the two poles of the cage and the remaining six tin atoms occupy the equator of the cage. The poles consist of trimeric O-capped subunits,  $[(n\text{-BuSn})_3(\mu_3\text{-O})(\mu\text{-OH})_3]$ . Within these subunits the tin atoms are hexacoordinate and possess bridging oxo and hydroxo groups. The equator of the cage is spanned by a hexameric organostannoxane cycle,  $[(n\text{-BuSn})_6(\mu_3\text{-O})_{12}]$ , containing  $[\text{Sn}_2(\mu\text{-O})_2]$  building blocks. In

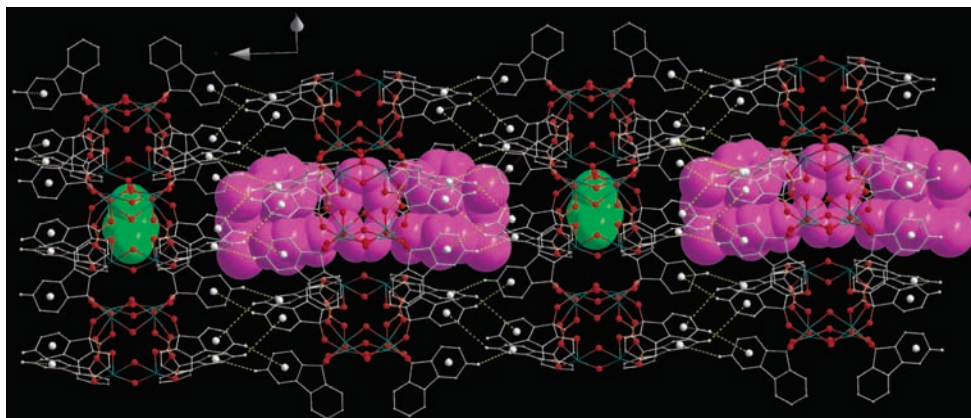
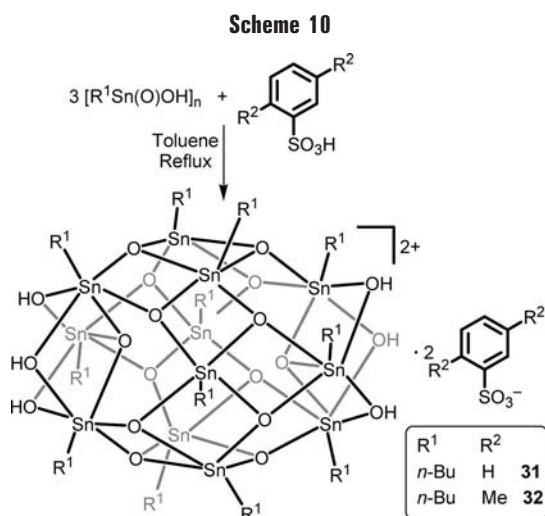


**FIGURE 8.** Hydrophobic and hydrophilic pockets in the supramolecular assembly of the compound **30**. Reproduced with permission from ref 19. Copyright 2005 American Chemical Society.



this subunit, the tin atoms are five-coordinate and are nearly square pyramidal. The diameter of the hexameric cyclic structural unit is 6.366(5) Å.

## Structural Interrelationship between Organostannoxane Cages

All the organostannoxane cages discussed in this Account have an intimate structural interrelationship. We will begin this discussion by first examining the important bond parameters found in these compounds, which are summarized in Table 1. For comparison, the structural parameters of a trinuclear O-capped cluster,  $\{[(n\text{-BuSn})_3(\mu_3\text{-O})(\mu\text{-OH})_3(\text{O}_2\text{PPh}_2)_3]^+[\text{Ph}_2\text{PO}_2]^- \}$ ,<sup>22</sup> are also given. The core structures of monoorganostannoxane cages such as the drum, the double O-capped cluster, and the football cage contain a  $\mu_3\text{-O}$ , which is formally an oxide ( $\text{O}^{2-}$ ) ligand.<sup>4</sup> The football cage and the double O-capped cluster also contain  $\mu\text{-O}$  in the form of hydroxide ( $\text{HO}^-$ ) or phenoxide ( $\text{RO}^-$ ) ligands. Similarly the O-capped cluster contains a  $\mu_3\text{-O}$  and a  $\mu\text{-OH}$ . In general, the Sn–O bond distances of the stannoxane cores do not vary much and are comparable in the various structural forms (Table 1). In the football cage, O-capped cluster, and double O-capped cluster, the Sn–( $\mu_3\text{-O}$ ) bond distance is found to be shorter than the

corresponding distance involving  $\mu\text{-O}$  (Table 1). The Sn– $\text{O}_{\text{exo-cage}}$  distance in all the cases is similar to the Sn–( $\mu\text{-O}$ )<sub>cage</sub> distance. The overall size of the drum ( $1.4 \times 1.8 \times 1.8 \text{ nm}^3$ ), the football cage ( $1.8 \times 1.8 \times 1.8 \text{ nm}^3$ ), the double O-capped cluster ( $1.6 \times 1.7 \times 1.8 \text{ nm}^3$ ), and the tetranuclear cage ( $1.3 \times 1.5 \times 1.8 \text{ nm}^3$ ) clearly indicates that these structural forms are nanodimensional.<sup>23</sup>

It is interesting to examine the formation of these cages from a structural point of view. Thus, the drums can be structurally assembled in at least five ways (Chart 4). Four of these involve the fusion of (a) two  $[\text{Sn}_2(\mu\text{-O})_2]$  four-membered rings with two Sn–O units, (b) three  $[\text{Sn}_2(\mu\text{-O})_2]$  four-membered rings, (c) two six-membered  $[\text{Sn}_3(\mu\text{-O})_3]$  rings, and (d) two O-capped clusters,  $[\text{Sn}_3(\mu_3\text{-O})(\mu\text{-OH})_3]$ , in a face-to-face manner. The fifth possibility is the folding of an open-chain hexanuclear ladder into a closed drum form. Two of these possibilities, the conversion of the open-chain ladder or the O-capped clusters into the drum, have been experimentally realized.<sup>4</sup> The football cage can be structurally assembled by coupling three  $[\text{Sn}_2(\mu\text{-O})_2]$  four-membered rings with two O-capped clusters (Chart 5). The double O-capped cluster can be formed by combining two O-capped clusters in a back-to-back manner with the assistance of four tridentate phosphonate ligands (Chart 5).<sup>13,14</sup> The tetranuclear cage is formed by the combination of two  $[\text{Sn}_2(\mu\text{-O})_2]$  units with eight  $[\text{RP}(\text{OH})\text{O}_2]^-$  ligands (Chart 5).<sup>7,8</sup>

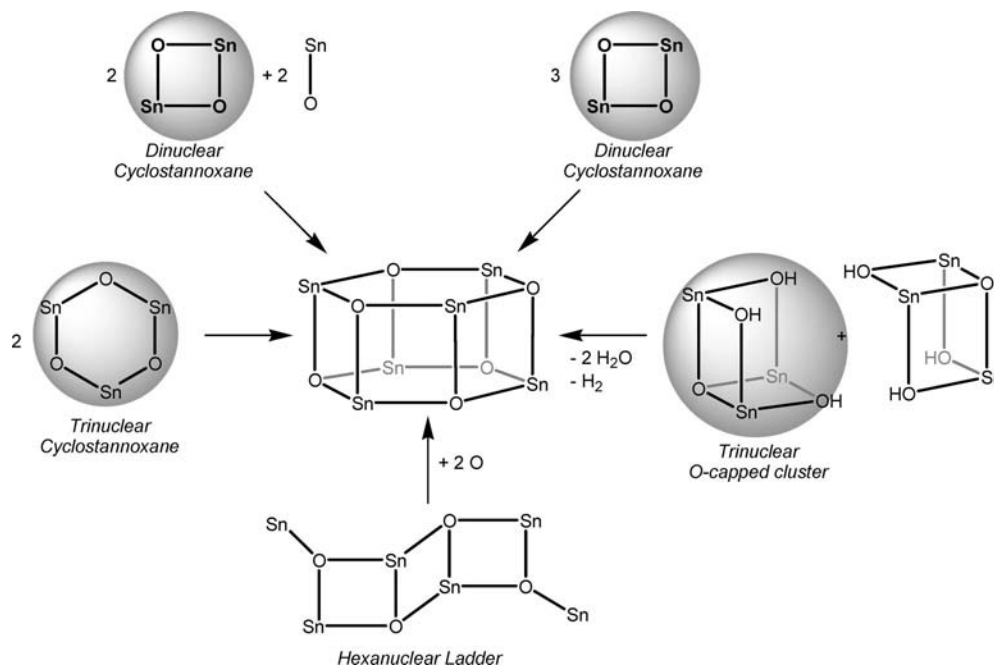
The intricate structural relationship between the drum, the football cage, and the double O-capped cluster becomes evident when one considers the following. As mentioned above, one of the ways of achieving the drum is by a face-to-face combination of two O-capped clusters,  $[\text{Sn}_3(\mu_3\text{-O})(\mu\text{-OH})_3]$  (Chart 4). If the two O-capped cluster cores are allowed to join back-to-back by the intervention of bridging  $[\text{HPO}_3]^{2-}$  ligands, the double O-capped cluster is obtained. If, instead of  $[\text{HPO}_3]^{2-}$  ligands, the two O-capped cluster cores are joined back-to-back by a central belt of  $\text{Sn}_6\text{O}_{12}$ , the football cage is formed (Chart 5).<sup>13,14</sup> Thus, it is clear that the football cage consisting of two poles (O-capped cluster) and an equator ( $\text{Sn}_6\text{O}_{12}$ ) is structurally very similar to the double O-capped clusters. This relationship is further emphasized by the bond



**Table 1. Average Bond Parameters for Various Nanodimensional Organostannoxane Compounds**

compound	structure	Sn-( $\mu_3$ -O) (Å)	Sn-( $\mu$ -OR) (Å)	Sn-O(X) (Å)	P...P <sup>a</sup> (Å)	( $\mu_3$ -O)...( $\mu_3$ -O) (Å)	ref
$\{[(n\text{-BuSn})_3(\mu_3\text{-O})(\mu\text{-OH})_3(\text{O}_2\text{PPh}_2)_3]^{+}[\text{Ph}_2\text{PO}_2]^{-}\}$	O-capped cluster	2.075(5)	2.128(6), R = H	2.122(6), X = P			22
$\{[(n\text{-BuSn})_3(\mu_3\text{-O})(\mu\text{-OPh})_3(\text{HPO}_3)_2]_2\}$ ( <b>21</b> )	double O-capped cluster	2.072(2)	2.172(2), R = Ph	2.072(2), X = P	6.337(1)	3.778(4)	13
$\{[(n\text{-BuSn})_{12}(\mu_3\text{-O})_{14}(\mu\text{-OH})_6]^{2+} \cdot 2(2,5\text{-Me}_2\text{C}_6\text{H}_3\text{SO}_3^{-})\}$ ( <b>32</b> )	football cage <sup>b</sup>	2.087(4)	2.110(5), R = H		6.366(5) <sup>e</sup>	3.955(5)	21
		2.117(4) <sup>c</sup>					
		2.059(4) <sup>d</sup>					
$[n\text{-BuSn}(\text{O})\text{O}_2\text{CC}_5\text{H}_4\text{FeC}_5\text{H}_5]_6$ ( <b>6</b> )	drum	2.087(6)		2.166(6), X = C			11a
$\{[(\text{BnSn})_2(\mu\text{-O})][\text{O}_2\text{P}(\text{OH})\text{-}t\text{-Bu}]_4\}_2$ ( <b>2</b> )	tetranuclear cage		2.117(2), R = O	2.079(2), X = P	6.311(2)	3.601(3) <sup>f</sup>	6

<sup>a</sup> Average distance between the diametrically opposite phosphorus atoms present in the equator. <sup>b</sup> Two crystallographically independent molecules are present. Bond parameters of only one molecule are given here. <sup>c</sup> Pole tin atoms bonded with  $\mu_3$ -oxygens, which are part of the equator. <sup>d</sup> Equator tin atoms bonded with  $\mu_3$ -oxygens, which are part of the equator. <sup>e</sup> Average distance between the diametrically opposite tin atoms present in the equator. <sup>f</sup> Distance between the diametrically opposite  $\mu$ -O atoms present in the poles.

**Chart 4. Structural Assembly of the Sn<sub>6</sub>O<sub>6</sub> Core of the Drum**

parameters found in these systems. The interpole distance of ( $\mu_3$ -O)...( $\mu_3$ -O) in **32** is 3.955(5) Å. In compounds **21–24**, this ranges from 3.778(4) to 3.825(9) Å. Similarly the distances between the diametrically opposite phosphorus atoms in **21–24** range from 6.274(5) to 6.337(1) Å. This is also comparable to the distance of diametrically opposite tin atoms in the central Sn<sub>6</sub>O<sub>12</sub> belt (equator) of the football cage **32** (6.366(5) Å) (Table 1). Although structurally distant, the internal geometric parameters of the tetranuclear cage are similar to those of the football cage and the double O-capped cluster. Thus, the interpole ( $\mu$ -O)...( $\mu$ -O) distance in the former is 3.601(3) Å, while the distance between the diagonally opposite phosphorus atoms of the central core is 6.311(2) Å.

## Solventless Synthesis

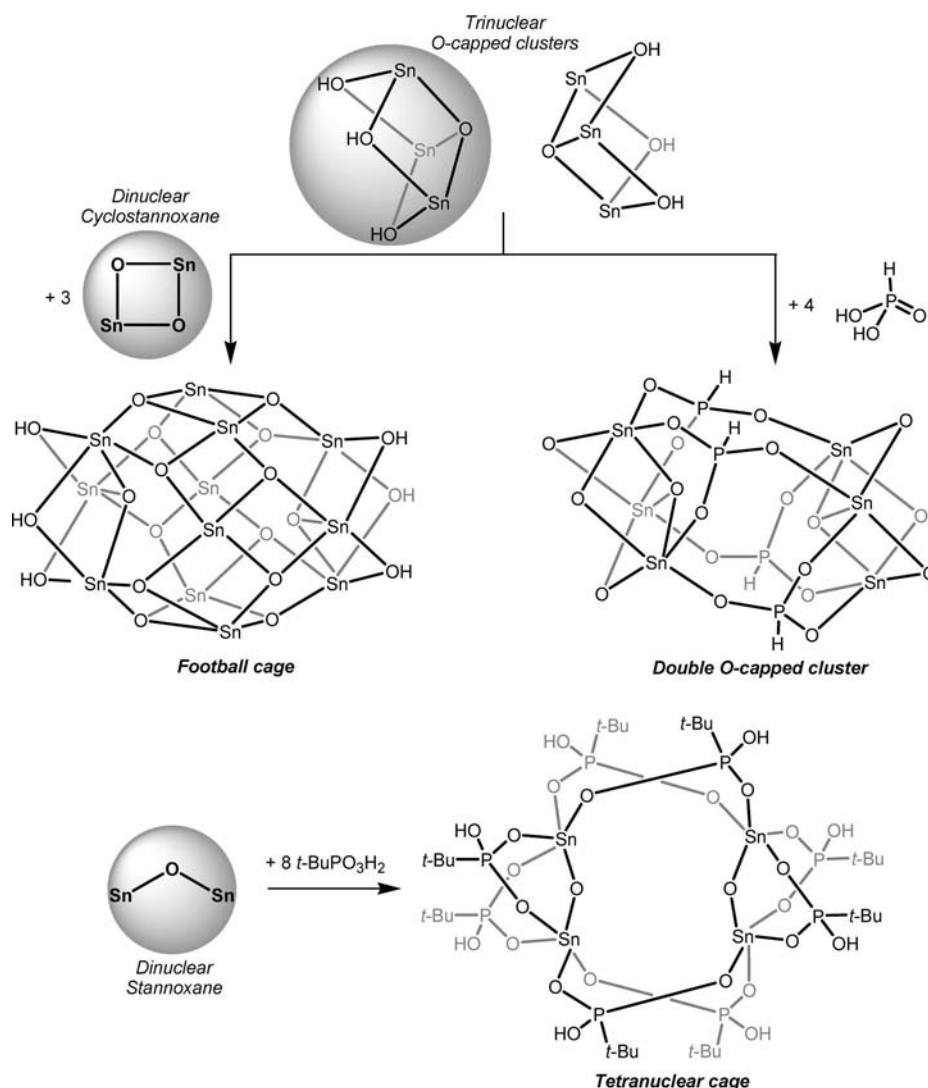
In addition to conventional synthetic procedures, recently, we have found that many different types of organotin compounds can be readily synthesized by a solid-state reaction, which involves grinding the reac-

tants together at ambient temperature. A variety of products can be prepared by this protocol with yields in excess of 90% (Scheme 11).<sup>11c</sup> In many cases, the progress of the reaction can be monitored by NMR. An interesting feature of this solid-state reaction is that during no stage of the reaction was a visible melt observed. It is believed that mechanical grinding provides sufficient contact between reactants to allow the reaction to occur. We were able to show by powder X-ray diffraction that crystallinity is maintained throughout the progress of the reaction.<sup>11c</sup>

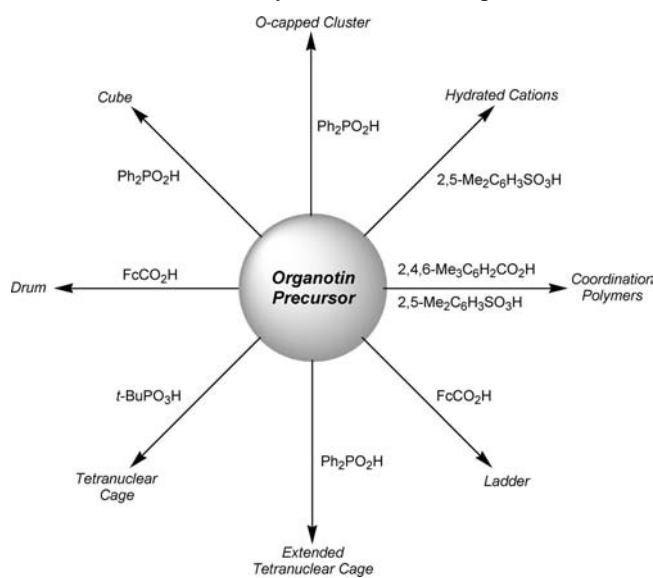
## Applications

The current state-of-the-art in the synthesis of organostannoxanes allows the assembly of any specific stannoxane cage or cluster exclusively. By a proper choice of the supporting ligands, it is possible to prepare dendrimer-like molecules containing a stannoxane core and a functional periphery. This strategy is detailed in the following sections.

Chart 5. Structural Assembly of the Various Stannoxane Cores



Scheme 11. Solventless Synthesis of Various Organostannoxanes

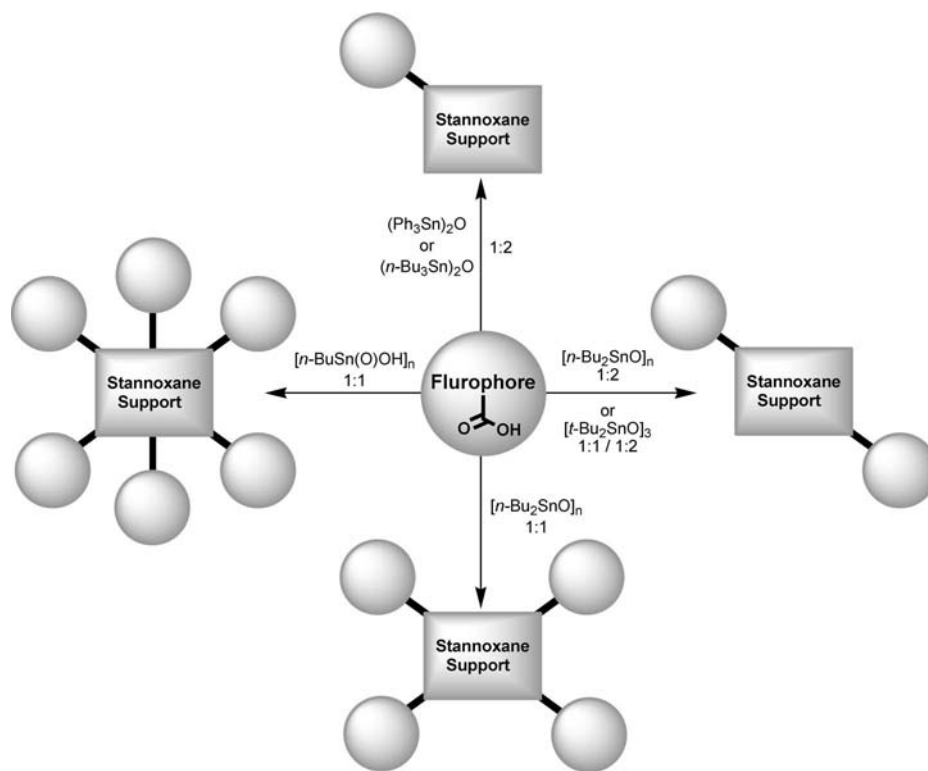


## Multi-photoactive Assemblies

Interest in photoactive compounds in new applications such as OLEDs, white-light emitters and in other optoelectronic applications<sup>24</sup> has spurred our interest in attempting to synthesize multi-photoactive assemblies supported on stannoxane cores. By choosing common fluorophores and by varying the organotin precursor we readily assembled a variety of photoactive compounds (Scheme 12, Table 2).<sup>11g</sup> The absorption spectra of these compounds are characterized by strong ligand centered  $\pi-\pi^*$  transitions. Their molar extinction coefficients show a strong dependence on the number of chromophores (Table 2). These compounds emit quite strongly when excited at their respective maximum absorption wavelengths. Thin-film photoluminescence of these compounds shows broad and red-shifted emission bands (Figure 9). This is due to the strong intermolecular interactions that occur between the chromophores in the solid-state (crystal structures of **27**, **28**, **33–35**, and **37** show rich supramolecular architectures due to the presence of intermolecular noncovalent interactions).<sup>11g</sup> The largest red shifts are seen for compounds containing six fluorenyl substituents.

It is noted that such broad features in the emission are of interest in white-light-emitting applications.<sup>24</sup>

## Scheme 12. Synthesis of Multi-photoactive Assemblies Supported on Stannoxane Cores



## Multiferrocene Assemblies

There is considerable interest in the assembly of multi-metallocene assemblies in general and multiferrocene compounds in particular. This is because of the potential applications of such compounds as electron reservoirs, electron-transfer mediators, electrode modification materials, ion sensors, etc.<sup>25</sup> In general, the synthetic procedures for the preparation of these compounds involve multistep protocols and the yields of the final product are generally modest. The stannoxane synthesis route allows assembly of multiferrocene compounds in a single step with high yields. In addition, the stannoxane cores are reasonably robust and do not interfere with the redox properties of the ferrocene groups. Further, the number

and orientation of the ferrocene ligands in the periphery can be easily modulated.<sup>17</sup>

Accordingly, compounds containing two, four, and six ferrocene derivatives were readily synthesized in nearly quantitative yields in one-step reaction protocols (Table 3).<sup>11a,11b,17</sup> A single quasi-reversible oxidation peak in their cyclic voltamogram (CV) characterizes the electrochemical behavior of these compounds (Table 3, Figure 10). The oxidation peak potentials are invariant and do not seem to be dependent on the stannoxane assembly or the number of the ferrocene units. Further, compounds **6**, **7**, **26**, and **40**, which contain the  $[\text{Sn}_2(\mu\text{-O})_2]$  units, do not show electrochemical decomposition in solution even after many continuous CV cycles testifying to the electrochemical stability of these assemblies.

The tendency to form supramolecular structures provides a basic route to self-assemble the stannoxane-supported ferrocene assemblies on predefined solid surfaces. The wetting behavior and electronic structure of **6** and **7** on a solid silicon surface has been recently demonstrated.<sup>26</sup>

## Multiporphyrin Compounds

Multiporphyrin arrays are of considerable interest as optoelectronic devices and in applications involving harvesting of light.<sup>27</sup> On the other hand, porphyrins are excellent ligands and the assembly of multiporphyrin assemblies allows the construction of multimetal compounds, which can be of interest in various catalytic applications. After ascertaining from quantum mechanical calculations that the hexameric stannoxane core ( $\text{Sn}_6\text{O}_6$ )

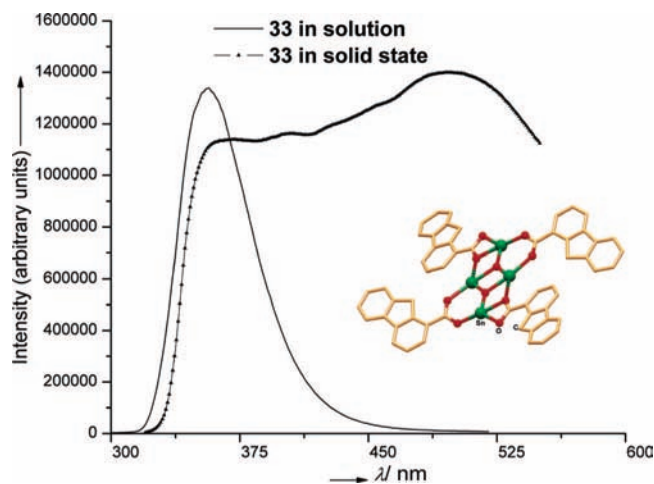
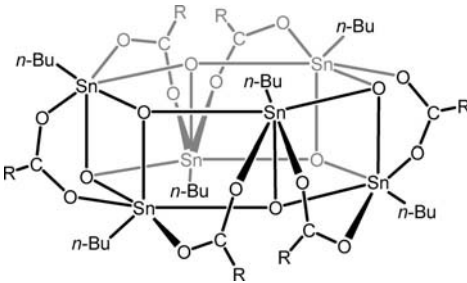
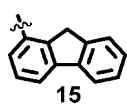
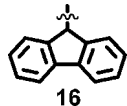
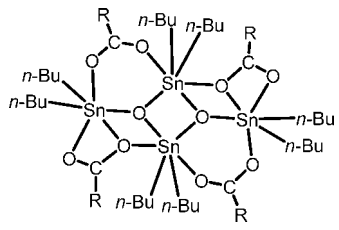
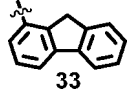
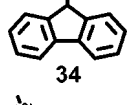
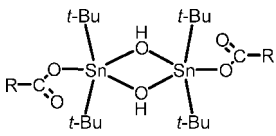
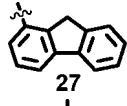
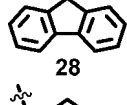
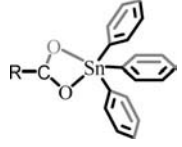
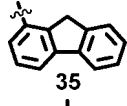
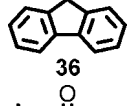
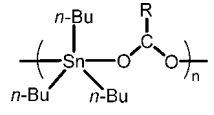
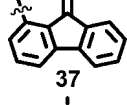
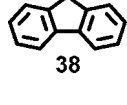


FIGURE 9. Solution and solid-state emission spectra of the tetrafluorene ladder **33**. Inset contains the molecular structure of **33**.

**Table 2. Photoluminescence Properties of Various Multi-photoactive Organostannoxane Compounds<sup>11g</sup>**

reactants	ratio	products	R	absorbance, $\lambda$ , nm ( $\epsilon_{\max} \times 10^4$ )	solution-state emission, $\lambda$ , nm	solid-state emission, $\lambda$ , nm
$[n\text{-BuSn}(\text{O}(\text{OH})_n + \text{R-CO}_2\text{H}]_n$	6:6		 <b>15</b>	265 (7.016); 313 (3.123)	355	370; 454; 500
			 <b>16</b>	290 (5.135)	380	495
$[n\text{-Bu}_2\text{SnO}]_n + \text{R-CO}_2\text{H}$	1:1		 <b>33</b>	265 (6.7298); 313 (2.164)	355	375; 450
			 <b>34</b>	290 (4.817)	390	505
$[t\text{-Bu}_2\text{SnO}]_3 + \text{R-CO}_2\text{H}$	1:3		 <b>27</b>	265 (5.694); 313 (2.620)	355	410
			 <b>28</b>	290 (4.284)	370	500
$[\text{Ph}_3\text{Sn}]_2\text{O} + \text{R-CO}_2\text{H}$	1:2		 <b>35</b>	265 (3.225); 313 (2.153)	355	375; 450
			 <b>36</b>	280 (3.342)	365	515
$[n\text{-Bu}_3\text{Sn}]_2\text{O} + \text{R-CO}_2\text{H}$	1:2		 <b>37</b>	275 (2.612); 325 (1.846); 400 (1.517)	355	340, 490
			 <b>38</b>	280 (3.152)	370	500

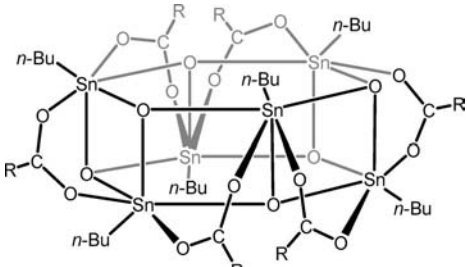
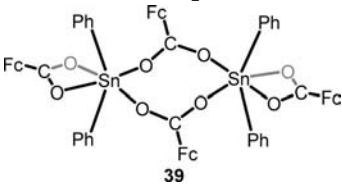
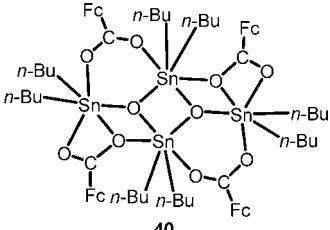
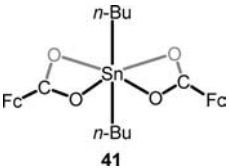
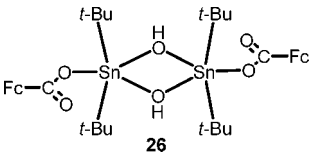
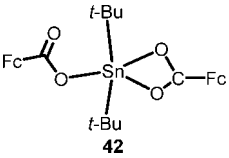
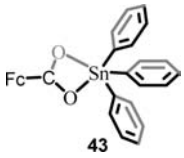
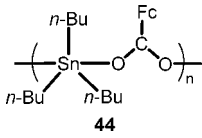
can support six porphyrin peripheral units (Figure 11), the synthesis of **18** was accomplished in nearly quantitative yields (Scheme 5).<sup>11d</sup> The hexa-metallated copper derivative **19** was shown to be a potent nuclease.<sup>11d</sup> Rapid DNA cleavage was achieved by **19** even in the absence of a co-oxidant. Further, **19** was found to be totally inactive towards protein cleavage, indicating the possibility of utilizing **19** for the selective removal of nucleic acid contaminants from cell extracts.

## Summary and Outlook

From the foregoing discussion on organooxotin cages, it is clear that these compounds are extremely interesting and possess diverse and varied structures. The preparation of organooxotin compounds is achieved by conventional procedures as well as by solventless methods. Organo-

stannoxane assemblies are quite adaptable in assuming various structural forms. However, despite their apparent dissimilarities, many organooxotin cages are structurally related to each other not only in their gross metrical parameters but also in the form of common building blocks. In most cases, the core structure of the organooxotin cage/cluster is supported by the additional coordination action of bridging multidentate oxygen-containing ligands such as carboxylates, phosphinates, or phosphonates. Because of their structural plasticity, changes in the ligand structure (nature and number of coordination sites) has a profound influence on the eventual structural form of the organooxotin assembly. There is, therefore, considerable opportunity to design and use new multidentate ligands to assist the formation of novel organooxotin cages and clusters.

**Table 3. Electrochemical Behavior of Various Multiferrrocene Organostannoxane Compounds**<sup>11a,11b,17</sup>

reactants <sup>a</sup>	ratio	products	$E_{1/2}$ (V)	$\Delta E_p$ (mV)
$[n\text{-BuSn}(\text{O})\text{OH}]_n + \text{R-CO}_2\text{H}$	6:6	 R=Fc- (6) R=FcCH <sub>2</sub> - (7)	+0.72 +0.50	128 240
$[\text{Ph}_2\text{SnO}]_n + \text{FcCO}_2\text{H}$	1:1 or 1:2	 39	+0.69	105
$[n\text{-Bu}_2\text{SnO}]_n + \text{Fc-CO}_2\text{H}$	1:1	 40	+0.73	184
	1:2	 41	+0.70	158
$[t\text{-Bu}_2\text{SnO}]_3 + \text{Fc-CO}_2\text{H}$	1:3	 26	+0.69	246
	1:6	 42	+0.65, +0.74	105, 92
$[\text{Ph}_3\text{Sn}]_2\text{O} + \text{Fc-CO}_2\text{H}$	1:2	 43	+0.66	106
$[n\text{-Bu}_3\text{Sn}]_2\text{O} + \text{Fc-CO}_2\text{H}$	1:2	 44	+0.57	112

<sup>a</sup> Fc = ferrocenyl, [(C<sub>5</sub>H<sub>5</sub>)Fe(C<sub>5</sub>H<sub>4</sub>)-].

The utility of organostannoxane synthesis in forming dendrimer-like structures containing a central stannoxane core and a functional periphery has been demonstrated. We are confident that this aspect of organostannoxane chemistry will receive much more attention in the future.<sup>25-28</sup> In addition, there have not been many reports thus far

about using organotin building blocks in building three-dimensional structures for assembling porous hybrid materials.

As mentioned above, most of the organostannoxane assemblies are prepared using organotin hydroxides and oxides as starting materials. Many of these starting materials

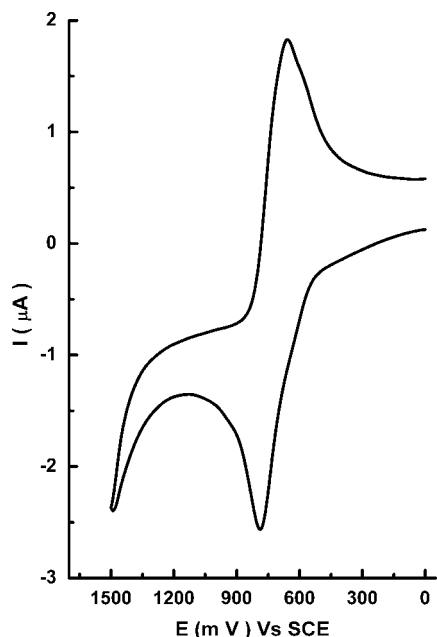


**FIGURE 10.** Cyclic voltammogram (CV) for the hexaferrocenyl drum 6.

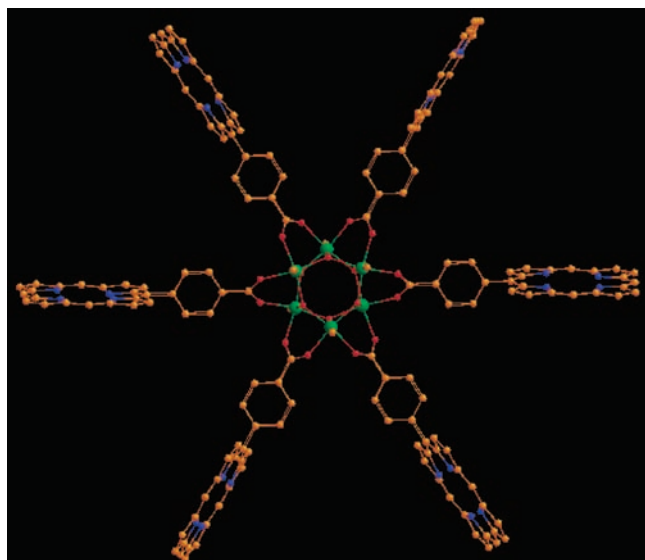


**FIGURE 11.** PM3-optimized geometry of the model compound  $[\text{MeSn}(\text{O})\text{O}_2\text{CC}_6\text{H}_4\text{-4-PH}_2]_6$  ( $\text{PH}_2 = 5\text{-}21,23\text{H-porphyrin}$ ). Reproduced with permission from ref 11d. Copyright 2005 American Chemical Society.

are not fully structurally characterized, and there is considerable scope in unraveling their mystery. There is no example of  $\text{RSn}(\text{OH})_3$  known thus far. The interesting chemistry arising from  $\text{RSi}(\text{OH})_3$ , as well as other main-group hydroxides such as  $\text{LAl}(\text{OH})_2$  or  $\text{LAl}(\text{OH})(\text{Me})$  ( $\text{LH} = [(2,6\text{-}i\text{-Pr}_2\text{-C}_6\text{H}_3)\{\text{NC}(\text{Me})\}_2\text{CH}]$ ),<sup>29</sup> warrant that serious efforts should be made to isolate this missing organotin congener. Availability of such precursors would pave the way for assembling novel heterometallic assemblies with interesting molecular structures and chemical reactivity.

We are thankful to the Department of Science and Technology and the Council of Scientific and Industrial Research, New Delhi, India, for supporting our research endeavor over a long period. V.C. is indebted to his co-workers, whose names are cited in the references, for their intellectual and experimental contributions.

## References

- (1) Davies, A. G. *Organotin Chemistry*, 2nd ed.; WILEY-VCH Verlag GmbH & Co. KGaA: Weinheim, Germany, 2004.
- (2) Otera, J. Toward ideal (trans)esterification by use of fluorous distannoxane catalysts. *Acc. Chem. Res.* **2004**, *37*, 288–296.
- (3) Gielen, M. Tin-based anti-tumor drugs. *Coord. Chem. Rev.* **1996**, *151*, 41–51.
- (4) (a) Chandrasekhar, V.; Nagendran, S.; Baskar, V. Organotin assemblies containing Sn–O bonds. *Coord. Chem. Rev.* **2002**, *235*, 1–52. (b) Holmes, R. R. Organotin cluster chemistry. *Acc. Chem. Res.* **1989**, *22*, 190–197.
- (5) Chandrasekhar, V.; Gopal, K.; Sasikumar, P.; Thirumoorthi, R. Organooxotin assemblies from Sn–C bond cleavage reactions. *Coord. Chem. Rev.* **2005**, *249*, 1745–1765.
- (6) Swamy, K. C. K.; Schmid, C. G.; Day, R. O.; Holmes, R. R. Organotin clusters. 6. Tetranuclear organooxotin cage compounds formed with phosphate and phosphonate ligands. A new class of organotin clusters. *J. Am. Chem. Soc.* **1990**, *112*, 223–228.
- (7) Chandrasekhar, V.; Baskar, V. Ligand driven assembly of a mono-organooxotin cage form the reactions of organotin precursors with phosphonate ligands. *Indian J. Chem.* **2003**, *42A*, 2376–2381.
- (8) Chandrasekhar, V.; Baskar, V.; Steiner, A.; Zacchini, S. Synthesis of a tetranuclear organooxotin cage by debenzoylation reactions: X-ray crystal structure of  $[(\text{PhCH}_2)_2\text{Sn}_2\text{O}(\text{O}_2\text{P}(\text{OH})\text{-t-Bu})_4]_2$ . *Organometallics* **2002**, *21*, 4528–4532.
- (9) Chandrasekhar, V.; Thirumoorthi, R.; Azhakar, R. New structural forms of organostannoxane macrocycle networks. *Organometallics* **2007**, *26*, 26–29.
- (10) Chandrasekhar, V.; Baskar, V.; Steiner, A.; Zacchini, S. Reactions of  $n\text{-Bu}_2\text{SnO}$  and  $(n\text{-Bu}_3\text{Sn})_2\text{O}$  with 1,1,2,3,3-pentamethyltrimethylene phosphinic acid: Synthesis and X-ray crystal structures of a novel spirocyclic coordination polymer and a 16-membered inorganic macrocycle. *Organometallics* **2004**, *23*, 1390–1395.
- (11) (a) Chandrasekhar, V.; Nagendran, S.; Bansal, S.; Kozee, M. A.; Powel, D. R. An iron wheel on a tin drum: A novel assembly of a hexaferrocene unit on a tin oxygen cluster. *Angew. Chem., Int. Ed.* **2000**, *19*, 1833–1835. (b) Chandrasekhar, V.; Nagendran, S.; Bansal, S.; Cordes, A. W.; Vij, A. Rangoli with tin drums: C–H...O bond-assisted supramolecular grids involving organostannoxane clusters. *Organometallics* **2002**, *21*, 3297–3300. (c) Chandrasekhar, V.; Baskar, V.; Boomishankar, R.; Gopal, K.; Zacchini, S.; Bickley, J. F.; Steiner, A. Solventless reactions for the synthesis of organotin clusters and cages. *Organometallics* **2003**, *22*, 3710–3716. (d) Chandrasekhar, V.; Nagendran, S.; Azhakar, R.; Kumar, M. R.; Srinivasan, A.; Ray, K.; Chandrasekhar, T. K.; Madavaiah, C.; Verma, S.; Priyakumar, U. D.; Sastry, G. N. A lipophilic hexaporphyrin assembly supported on a stannoxane core. *J. Am. Chem. Soc.* **2005**, *127*, 2410–2411. (e) Chandrasekhar, V.; Gopal, K.; Nagendran, S.; Steiner, A.; Zacchini, S. Influence of aromatic substituents on the supramolecular architectures of monoorganooxotin drums. *Cryst. Growth Des.* **2006**, *6*, 267–273. (f) Chandrasekhar, V.; Thilagar, P.; Sasikumar, P. Multi-site coordination ligands assembled on organostannoxane supports. *J. Organomet. Chem.* **2006**, *691*, 1681–1692. (g) Chandrasekhar, V.; Thilagar, P.; Steiner, A.; Bickley, J. F. Inorganic-cored photoactive assemblies: Synthesis, structure, and photochemical investigations on stannoxane-supported multifluorene compounds. *Chem.—Eur. J.* **2006**, *12*, 8847–8861.
- (12) Day, R. O.; Chandrasekhar, V.; Swamy, K. C. K.; Holmes, J. M.; Burton, S. D.; Holmes, R. R. Organotin clusters. 3. Novel drums and mixed-drum organooxotin clusters from carboxylic, phosphinic, and phosphoric acids. *Inorg. Chem.* **1988**, *27*, 2887–2893.
- (13) Chandrasekhar, V.; Baskar, V.; Vittal, J. J. A new structural form of tin in a double O-capped cluster. *J. Am. Chem. Soc.* **2003**, *125*, 2392–2393.
- (14) Chandrasekhar, V.; Baskar, V.; Gopal, K.; Vittal, J. J. Organooxotin cages,  $\{[(n\text{-BuSn})_3(\mu_3\text{-O})(\text{OC}_6\text{H}_4\text{-4-X})_3]_2[\text{HPO}_3]_4\}$ , X = H, Cl, Br, and I, in double O-capped structures: Halogen-bonding-mediated supramolecular formation. *Organometallics* **2005**, *24*, 4926–4932.
- (15) Metrangolo, P.; Neukirch, H.; Pilati, T.; Resnati, G. Halogen bonding based recognition processes: A world parallel to hydrogen bonding. *Acc. Chem. Res.* **2005**, *38*, 386–395.

- (16) Chandrasekhar, V.; Nagendran, S.; Gopal, K.; Steiner, A.; Zacchini, S. First example of a Sn–C bond cleaved product in the reaction of  $\text{Ph}_3\text{SnOSnPh}_3$  with carboxylic acids. 3D-Supramolecular network formation in the X-ray crystal structure of  $[\text{Ph}_2\text{Sn}(\text{OH})\text{OC}(\text{O})(\text{R}_f)]_2$ ,  $\text{R}_f = 2,4,6\text{-(CF}_3)_3\text{C}_6\text{H}_2$ . *Chem. Commun.* **2003**, 862–863.
- (17) Chandrasekhar, V.; Gopal, K.; Nagendran, S.; Singh, P.; Steiner, A.; Zacchini, S.; Bickley, J. F. Organostannoxane-supported multi-ferrocenyl assemblies: Synthesis, novel supramolecular structures, and electrochemistry. *Chem.—Eur. J.* **2005**, *11*, 5437–5448.
- (18) Sakamoto, K.; Ikeda, H.; Akashi, H.; Fukuyama, T.; Orita, A.; Otera, J. Synthesis and structural studies on dimeric organotin cations. *Organometallics* **2000**, *19*, 3242–3248.
- (19) Chandrasekhar, V.; Thilagar, P.; Steiner, A.; Bickley, J. F. Alternating hydrophilic and hydrophobic pockets in the channel structures of organostannoxane prismanes: Preferential confinement of guest molecules. *J. Am. Chem. Soc.* **2005**, *127*, 11556–11557.
- (20) Banse, F.; Ribot, F.; Tolédano, P.; Maquet, J.; Sanchez, C. Hydrolysis of monobutyltin trialkoxides: Synthesis and characterizations of  $\{(n\text{-BuSn})_{12}\text{O}_{14}(\text{OH})_6\}(\text{OH})_2$ . *Inorg. Chem.* **1995**, *34*, 6371–6379.
- (21) Chandrasekhar, V.; Boomishankar, R.; Gopal, K.; Sasikumar, P.; Singh, P.; Steiner, A.; Zacchini, S. Synthesis, structure and reactivity of hydrated and dehydrated diorganotin cations. *Eur. J. Inorg. Chem.* **2006**, 4129–4136.
- (22) Day, R. O.; Holmes, J. M.; Chandrasekhar, V.; Holmes, R. R. A new structural form of tin in an oxygen-capped cluster. *J. Am. Chem. Soc.* **1987**, *109*, 940–941.
- (23) These dimensions represent end to end proton distances.
- (24) Richter, M. M. Electrochemiluminescence (ECL). *Chem. Rev.* **2004**, *104*, 3003–3036.
- (25) Chase, P. A.; Gebbink, R. J. M. K.; van Koten, G. Where organometallics and dendrimers merge: The incorporation of organometallic species into dendritic molecules. *J. Organomet. Chem.* **2004**, *689*, 4016–4054.
- (26) Frehill, F.; Schulte, K. H. G.; Martin, C. P.; Wang, L.; Patel, S.; Purton, J. A.; Vos, J. G.; Moriarty, P. Iron wheels on silicon: Wetting behavior and electronic structure of adsorbed organostannoxane clusters. *Langmuir* **2004**, *20*, 6421–6429.
- (27) Kim, D.; Osuka, A. Directly linked porphyrin arrays with tunable excitonic interactions. *Acc. Chem. Res.* **2004**, *37*, 735–745.
- (28) Hahn, U.; Gegout, A.; Duhayon, C.; Coppel, Y.; Saquet, A.; Nierengarten, J.-F. Self-assembly of fullerene-rich nanostructures with a stannoxane core. *Chem. Commun.* **2007**, 516–518.
- (29) Roesky, H. W.; Singh, S.; Janick, V.; Chandrasekhar, V. A paradigm change in assembling OH functionalities, on metal centers. *Acc. Chem. Res.* **2004**, *37*, 969–981.

AR600061F